Volume 16, Issue 2, 162516 (1-16)

International Journal of Nano Dimension (IJND)

https://doi.org/10.57647/j.ijnd.2025.1602.16

Development and optimization of polymeric nanosponges for enhanced delivery of diflunisal in rheumatoid arthritis

Kiran Balasaheb Aher[1,*], Shubham Bhosale[1], Girija Balasaheb Bhavar [2], Mohammad Habeeb[3,*], Huay Woon You[4]

[1]*Department of Pharmaceutical Quality Assurance, Shri Vile Parle Kelavani Mandal's Institute of Pharmacy, Dhule, Maharashtra, India.*
[2]*Department of Pharmaceutical Chemistry, Shri Vile Parle Kelavani Mandal's Institute of Pharmacy, Dhule, Maharashtra, India.*
[3]*Department of Pharmaceutics, Crescent School of Pharmacy, B.S. Abdur Rahman Crescent Institute of Science and Technology, Chennai, India.*
[4]*Pusat PERMATA@Pintar Negara, Universiti Kebangsaan Malaysia, Bangi, Selangor, Malaysia.*

[*]**Corresponding authors:** aherkiran22@gmail.com; mdhabeebqa@gmail.com

Original Research

Received:
29 July 2024
Revised:
3 November 2024
Accepted:
9 November 2024
Published online:
1 April 2025

Abstract:

Rheumatoid arthritis damages the synovial membrane, and diflunisal, a nonsteroidal anti-inflammatory drug (NSAID) with poor solubility, faces delivery challenges. nanosponges enhance diflunisals solubility improving its bioavailability; in addition it improved its stability and controls its release. Current research focuses on developing polymeric nanosponges (DIF-NS) through emulsion solvent evaporation, optimized by central composite design. The optimized DIF-NS were further loaded into a carbopol 940 gel (DIF-NS-gel) and evaluated. The optimized BNS showed spherical morphology, % CDR (Percentage cumulative drug release) of 84.9 ± 1.6 within 12 hours and % entrapment efficiency of 82.45 % ± 1.2, a % practical yield of 75 % ± 2.2 with a particle size of 120.1 ± 8.5 nm, zeta potential -29 ± 3.2 mv, and a PDI of 0.348 ± 0.015. The drug excipient compatibility study was carried out by using FTIR. The sharp peak obtained in the DSC and XRD proves the drug's crystalline nature. The DIF-NS-gel exhibited sustained release and enhanced ex-vivo permeation compared to plain diflunisal gel. In a CFA-induced rheumatoid arthritis rabbit model, it significantly reduced inflammation for a prolonged duration. These findings highlight its potential for effective long-term rheumatoid arthritis management.

Keywords: Diflunisal; Drug delivery; Nanosponges; Rheumatoid arthritis; Statistical optimization

1. Introduction

Rheumatoid arthritis is a chronic, systemic autoimmune disorder characterized by persistent inflammation, primarily targeting the joints but also affecting other organs and tissues. The exact cause remains unknown [1]. Rheumatoid arthritis is the most prevalent disease mostly affecting between 0.5% and 1% of adults worldwide, and its prevalence varies from region to region. North America and Europe have a higher prevalence than Asia [2]. In China, about 0.42% of the population suffers from rheumatoid arthritis, making it an emerging significant health concern. Notably, it has developed the primary reason of physical frailty in Chinese women and ranks among the top 10 prevalent chronic conditions in the country [3]. The occurrences of rheumatoid arthritis are 2 times higher in men than in women. Although the disease can arise at any age, it is utmost communal in people amongst 40 and 70 years old, as its incidence increases with age [4]. From 1980 to 2019, the prevalence increased from 0.46% to 0.53%, affecting a probable 17.6 million people worldwide in 2020 [5]. Despite a decrease in rheumatoid arthritis mortality over the past three periods, global age-standardized pervasiveness rates have continued to rise, and the number of cases will increase in 2050. Enhanced access to first diagnosis and treatment is necessary to reduce the disease's future burden. Treatment tactics for rheumatoid arthritis include the consumption of non-steroidal anti-inflammatory drugs (NSAIDs) as well as immunosuppressants with a higher dose in severe conditions. If the joints suffer greatly then surgery is the last

option in front of patients [6]. The treatment of rheumatoid arthritis involves non-steroidal anti-inflammatory drugs (NSAIDs) like ibuprofen, naproxen, and diclofenac with dosages ranging from 2.5 to 10 mg/day for most patients. However, higher doses of 400 to 800 mg/day may be required in severe cases. These drugs are highly preferred for oral route of administration [7]. Diflunisal (DIF), a derivative of salicylic acid, is classified as a non-selective COX inhibitor. DIF, classified under the BCS class-II, possesses remarkable anti-inflammatory properties and is marketed as DOLOBID for the long-term management of rheumatoid arthritis. The oral dose of the DIF is 250 mg to 500 mg respectively. Although DIF is frequently used to treat rheumatoid arthritis, its conventional tablet formulation exhibits minimum bio availability due to the various Gastrointestinal barriers [8]. When administered orally, these non-steroidal anti-inflammatory drugs (NSAIDs) exhibit significant toxic effects, including cardiovascular complications, renal impairment, gastrointestinal toxicity, thrombocytopenia, hepatotoxicity, hypertension, and other minor health issues non-steroidal anti-inflammatory drugs (NSAIDs) show heavy toxic effects when taken by the oral route of administration encompassing cardiovascular risks, renal damage, and gastrointestinal toxicity, thrombocytopenic and liver toxicity as well as hypertension and other slight ailments [9, 10] That' s why researchers have developed topical approaches for treating rheumatoid arthritis. In the context of our research, the QbD framework guides the optimization of nanosponges preparation, ensuring that the CMPs (EC and PVA) are precisely controlled to achieve the desired CQAs such as Y1 = % Drug Diffusion (% DD), Y2 = % Entrapment Efficiency (% EE), Y3 = Particle Size (PS), Y4 = % Practical Yield (% PY) [10]. This methodology not only enhances the reproducibility of the nanosponge formulation but also ensures that the final product meets the stringent quality standards required for effective drug delivery [11]. Additionally, a diversity of nanotechnology-based topical designs has been advanced like liposomes, nanoemulsion, nanoparticles, nano-Lipidic Carriers, nanosponges, nanocapsule, nonosuspension, nanofibers, nanocrystal etc [12, 13]. Despite the advantages and limitations of other topical delivery carriers, nanosponges have captured significant attention to their three-dimensional design, extensive drug loading capacity, and ability to encapsulate and distribute various drugs within their porous nanostructure [13]. Exploring innovative drug delivery systems like nanosponges is crucial for overcoming the limitations of traditional treatments, which often suffer from poor bioavailability and undesirable side effects, particularly in the case of orally administered non-steroidal anti-inflammatory drugs (NSAIDs) [14]. Recent studies have shown that nanoformulations can significantly enhance the pharmacokinetic profiles of anti-inflammatory drugs, leading to more efficient and sustained therapeutic outcomes [15]. The development of topical drug delivery systems like nanosponges aligns with the ongoing shift towards targeted and localized therapy, which aims to reduce systemic exposure and associated toxicities [16]. This approach is especially relevant in managing chronic inflammatory diseases like rheumatoid arthritis, where long-term medication use can result in severe side effects [17]. The adoption of nanotechnology in drug delivery is driven by the need to achieve controlled drug release, increase drug stability, and improve patient compliance. These factors underscore the significance of research efforts focused on enhancing the effectiveness of conventional drugs through nanotechnology-based formulations [18]. Nanosponges are in nano-size consisting of a polymer matrix characterized by nanocavities and molecular hyper-crosslinking between polymer and cross-linker [19].

Using nanosponges in diflunisal delivery for rheumatoid arthritis, it is essential to highlight their unique benefits. Nanosponges possess a porous structure and large surface area that enable efficient encapsulation and improved solubility of poorly soluble drugs like diflunisal. They protect the drug from degradation and facilitate enhanced permeability across biological membranes, ensuring controlled and sustained drug release for steady plasma levels. This targeted approach minimizes systemic exposure and associated toxicities, addressing side effects common with chronic NSAID use. Unlike other delivery systems such as liposomes and nanoemulsions, nanosponges provide superior drug-loading capacity and compatibility for both hydrophilic and hydrophobic drugs, promoting effective drug distribution. This results in better patient compliance and overall improved therapeutic outcomes by reducing adverse effects and enhancing treatment efficacy [20]. They are comparatively straightforward to fabricate equated to nano-suspensions or nano-emulsions and can be readily upscaled for manufacturing production [21]. Previously different types of nanoformulations of DIF were developed by the researcher such as nanoemulsion, liposomes, and nano-engineered lipidic carriers, etc [22]. These formulations have also been assessed for their physicochemical characteristics, including particle size, percentage entrapment efficiency, and zeta potential. Furthermore, researchers investigated Ex-vivo and In vitro models demonstrating sustained release behavior. This study aimed to develop DIF-loaded nanosponges to enhance skin membrane permeation, achieving prolonged drug release for effective rheumatoid arthritis treatment.

2. Material and methods

DIF (98%) was acquired from Otto Chemie Pvt Ltd., Mumbai. Ethyl Cellulose (7cps) (EC), Polyvinyl Alcohol (PVA), and Carbopol 940 were sourced from Research Lab, Mumbai. Cellophane was purchased from HiMedia Laboratories, Mumbai, India. Double distilled water, essential for the formulations, was prepared using an in-house double distillation unit. Acetonitrile and methanol were sourced from Merck, while potassium dihydrogen phosphate was obtained from Ranchem Pvt Ltd Mumbai. Complete Freund's adjuvant (CFA) was purchased from SIGMA-ALDRICH (F5881-10 mL) (PCode 1003552933; SLCN3573), stored at 2 to 8 ^{O}C, and used to induce arthritis in rats.

2.1 Optimization of diflunisal nanosponges

The optimization of DIF-loaded nanosponges was carried out through Response Surface Methodology (RSM) using

Table 1. Different independent and dependent variables for CCD.

Variables	Level		
	LOW (-1)	**Medium (0)**	**High (+1)**
Independent Variables			
A = Ethyl Cellulose (mg)	75	100	125
B = PVA (mg)	60	90	120
Dependent Variables			
Y1 = % Drug diffusion (% DD)		Y3 = Particle size (PS)	
Y2 = % Entrapment efficiency (% EE)		Y4 = % Practical yield (% PY)	

a Central Composite Statistical Design, facilitated by Design Expert® software, version 13. This approach aimed to understand the relationship between various factors influencing product quality and its critical attributes. Specifically, the impact of factors like EC (A) and PVA (B) on parameters such as % DD (Y1), % EE (Y2), PS (Y3), and % PY (Y4) of DIF-NS was investigated. The study involved evaluating the effects of these factors across different levels, with particle size targeted for minimization and % EE, % DD, and % PY aimed at maximization. The proposed statistical design included 11 experimental runs, incorporating three sovereign variables at three echelons each, to evaluate their discrete, interactive, and quadratic impacts on the reliant on variables. Table 1 shows both independent and reliant on variables, including their echelons and the measured responses from the experimental runs [23].

2.2 Formulation of diflunisal nanosponges

Nanosponges of diflunisal were fabricated using a technique called emulsion solvent evaporation method with a high-speed homogenization which is shown in Fig. 1. The First step is the mixing of DIF and EC in dichloromethane. After that, it was carefully dripped into a water-based solution of PVA (acting as a stabilizer) by means of a high-speed homogenizer (IKA T25 Digital Ultra Turrax) for 30 min. at 15000 rpm. The blend was left to stir on a magnetic stirrer for 3 hours at 1000 rpm to let the organic solvent evaporate completely. Next, the mix was rotated in a centrifuge at 14000 rpm and 4 ^{O}C for 30 minutes using a REMI R8K centrifuge. The resulting nanosponges were collected, dried properly, and kept safe for further examination [24].

2.3 Development of topical gel impregnated with DIF-NS

A total of four DIF-NS-gel batches, labelled G1 to G4, were formulated with varying concentrations of carbopol 940P, from 0.5% to 2%. Carbopol 940P was firstly drenched in water for 24 hours, then mixed thoroughly at 1000 rpm using a magnetic stirrer. To adjust the pH, 2% (v/v) Triethanolamine was added. Propylene glycol and N-methyl-2-pyrrolidone were then incorporated as permeation accompaniments. Methyl paraben (0.1%) and propyl paraben (0.01%) were dissolved in 10 mL of distilled water and subsequently incorporated into the carbopol 940P solution, which was then stirred at 500-800 rpm until the dispersion was smooth. After allowing the viscous mixture to sit undisturbed for 30 minutes, it was neutralized with 2% (v/v) Triethanolamine. Following this, ethanoic solutions of DIF (0.5%) and DIF-NS (0.5% w/w equivalent to DIF) were added to create the DIF-loaded gel (Plain Gel) and DIF-NS-gel, respectively. The prepared gels were then stored in aluminium tubes at room temperature. The alignments of the gels are tabulated in Table 2 [25].

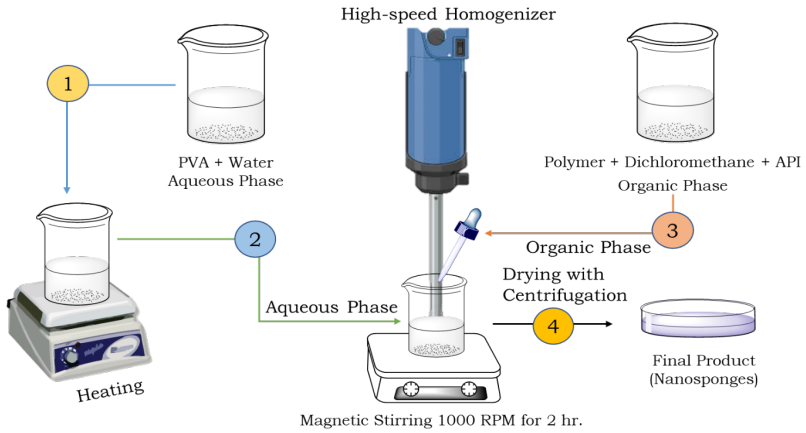

Figure 1. Preparation of nanosponges by high-speed homogenization method.

Table 2. Batches of gel formulation.

Ingredients	G1	G2	G3	G4
Carbopol 940P	0.5%	1%	1.5%	2%
Drug Concentration	0.5%	0.5%	0.5%	0.5%
Propylene glycol	2.5%	2.5%	2.5%	2.5%
Triethanolamine	q.s	q.s	q.s	q.s
Methyl paraben	0.10%	0.10%	0.10%	0.10%
Propyl paraben	0.01%	0.01%	0.01%	0.01%
Distilled Water	q.s	q.s	q.s	q.s

2.4 Evaluation and characterization of DIF-NS

2.4.1 Fourier transform infrared spectroscopy (FTIR)

The FTIR spectra for various recipients, including pure DIF, Blank-NS, and DIF-NS, were obtained using an FTIR spectrometer (PerkinElmer Ultra Two). The spectra were recorded over a wavenumber range from 4000 to 400 cm^{-1}. A small amount of each sample was placed on a diamond crystal, and pressure was applied to ensure proper contact, while energy levels were verified. To assess physical compatibility, the drug was mixed with the excipients in a 1:1 ratio and subjected to different physical conditions, including UV light exposure, high temperatures up to 500 ^{O}C, and accelerated stability conditions (40 $\pm$ 2 ^{O}C and 75% $\pm$ 5% relative humidity). For the chemical compatibility study, the excipients were mixed with DIF in a 1:1 ratio and stored for 180 days, with periodic IR spectroscopy readings taken throughout this period [26].

2.4.2 Differential scanning calorimetry

Differential Scanning Calorimetry (DSC) was utilized to assess the explicit heat capacity of various samples. This involved using a DSC instrument (Model DSC 823, Mettler Toledo). In this study, the samples encompassed pure diflunisal, Blank-NS, and DIF-NS. Each sample, about 10 mg in weight, was carefully positioned on an aluminium pan and wrapped tightly. Then exposed the tasters to heated, while purging gas (at a rate of 10 ml/min) was flowed over them, gradually increasing the temperature from 25 to 300 ^{O}C at a rate of 10 ^{O}C/min. Additionally, to provide a baseline for comparison, we placed a sealed empty pan alongside the samples and recorded the resulting thermogram [27].

2.4.3 X-ray diffractometry

The X-ray diffraction patterns for both pure DIF and DIF-NS were documented by means of a wide-angle X-ray scattering instrument (D 8 Advance Bruker, Germany). The tasters were secured onto a receptacle and rotated at a speed of 1 degree per minute. The resulting bands were contrived, representing scattering intensity against the 2θ angle [28].

2.4.4 Analysis by RP-HPLC

The HPLC investigation of diflunisal, a reversed-phase C18 column (Bridge@ C18; 250 mm $\times$ 4.6 mm I. D. , 5 μm) was employed, utilizing a Water Alliance RP-HPLC system (Waters e2695) controlled by Empower 3 software. The mobile phase included acetonitrile, distilled water, and phosphate buffer (0.025 M, pH 3.5) in the proportions of 60 : 30 : 10, with a flow rate of 1 mL/min. A 10 μL taster was injected, and the UV detector monitored the eluent at 258 nm. The retention time was 5.5 $\pm$ 0.24 minutes, with isocratic elution at an ambient temperature of 25 ^{O}C [29, 30].

2.4.5 Zeta potential, particle size, and polydispersity index

Particle size signifies the measurements of the individual particles covering all formulations. The DIF-NS underwent particle size analysis using the HORIBA SCIENTIFIC SZ-100 particle size analyzer (Version 2.40). To achieve the intended scattering intensity, the samples were diluted with water that had been double-distilled. Likewise, the zeta potential was determined using the Zetameter (HORIBA SCIENTIFIC SZ-100, Ver. 2.40). All measurements were conducted in triplicate for accuracy [31].

2.4.6 Percentage entrapment efficiency and percentage practical yield

Two methods are typically employed to find out entrapment efficiency and yield: indirect and direct methods. In this investigation, the direct method was utilized to determine % EE. In this study, the quantity of DIF-NS was accurately weighed and dispersed in a suitable solvent favourable to drug solubility. Subsequently, 10 mL of the solution was extracted and centrifuged at 5000 rpm, at a temperature of 4 ^{O}C for 30 min. The resulting supernatant was poised, riddled, and subjected to analysis using spectroscopy. % EE was calculated using Equation 1, while yield was computed using Equation 2 [32].

$$\%EE = \frac{\text{Drug Concentration in the formulation}}{\text{Total Amount of drug in the formulation}} \times 100 \quad (1)$$

$$\%PY = \frac{\text{Total weight of nanosponges}}{\text{Total weight of nanosponges}} \times 100 \quad (2)$$

2.4.7 Field emission scanning electron microscopy (FE-SEM)

FESEM exploited to examine the peripheral morphology and characteristics of DIF-NS. The sample was coated with a gold-palladium layer under ambient conditions before being examined with a SEM (Nova Nano SEM NPEB303) at 5000 x magnification in an argon environment [33].

2.5 Evaluation of DIF-NS gel

2.5.1 pH and visual appearance

The physical characteristics, including color and clarity, were documented through visual inspections. The pH level of the DIF-NS loaded gel was determined with a calibrated pH meter. (Equiptronics–EQ-610).

2.5.2 Measurement of viscosity:

The viscosities of the gel were measured by means of a Brookfield viscometer (Ametek DVPLLV) with spindle 62. The viscosity determination involved rotating the spindle at various angular velocities for a set time period of 1 minute to obtain the apparent viscosity.

2.5.3 Determination of spreadability:

To determine gel spreadability, place a defined amount of gel on a horizontal surface. Apply a standard weight on top for a set time. Measure the diameter of the spread area perpendicular to the direction of the applied force. Calculate spreadability using the Equation 3 [34].

$$\text{Spreadability} = \frac{\text{Spread diameter}}{\text{Initial weight applied}} \times 100 \quad (3)$$

2.5.4 In vitro drug release study:

In vitro drug release DIF-NS in the topical gel, DIF-NS, and Simple DIF dispersed gel was determined using Frans diffusion cell. The cellophane membrane is soaked in PBS pH 7.4 overnight. The receptor chamber consists of PBS pH 7.4 as dissolution media and the donor cubicle consists of DIF-NS loaded carbopol gel. The cellophane membrane was carefully positioned without disturbance, and the temperature was kept at 37 $\pm$ 2 ^{O}C with a stirring speed of 100 RPM. An *in vitro* drug release investigation was steered over 12 hours, with 1 mL samples withdrawn from the receptor partition at specific interludes (0.5, 1, 2, 3, 4, 5, 6, 8, 9, 10, 11, and 12 hours). To preserve sink situations, the quiet volume was replaced with renewed media. The tasters were then analyzed using UV spectroscopy at 258 nm.

2.5.5 Ex-vivo permeation study:

An ex-vivo drug permeation investigation was conducted utilizing Franz diffusion cells, featuring a 10 ml receiver cell volume and a permeation area of 0.185 cm^2. Skin from an albino rat was used as the permeation barrier. The donor compartment contained the gel, positioned above the receptor section full with PBS (pH 7.4). The rat skin was placed between the compartments and secured with a clamp. The experiment ran for 12 hours at 37 $\pm$ 2 ^{O}C with continuous magnetic stirring. Samples were taken from the receptor cell at predetermined interludes (0.5, 1, 2, 3, 4, 5, 6, 8, 9, 10, 11, and 12 hours) and analyzed for DIF content using a UV spectrophotometer at 288 nm. The data collected enabled the determination of skin parameters such as flux (J, μg/cm^2/h) and cumulative permeation.

2.5.6 Determination of release kinetics model

The drug release mechanism was examined by smearing innumerable mathematical models, together with Zero-order, First-order, Higuchi, and Korsemeyer-Peppas, to the collected data. The replicas were evaluated and equated by analysing the constant of determination (R^2) obtained through regression analysis. The model with the best fit, indicated by the highest R2 value, was selected to describe the release mechanism of DIF from the nanosponge matrix.

2.5.7 Stability study

The stability assessment of the DIF-NS topical gel batch was achieved to assess the possessions of formulation additives on DIF-NS-gel stability and to determine the physical constancy of the formulation. The stability study included various storage conditions and temperatures. The optimized batch formulation was exposed to accelerated stability state 40 ^{O}C $\pm$ 2 ^{O}C / 75% RH $\pm$ 5% RH as well as in a photostability chamber. Samples were collected at specific intervals (30, 60, 90, 120, 150, and 180 days) for physical evaluation, including measurements of pH, colour, odour and drug content.

2.6 Animal study

All animal trials were agreed out in amenability with the rules established by the Institutional Animal Ethical Committee (IAEC) of Shri Vile Parle Kelavani Mandal's Institute of Pharmacy. The IAEC is registered under the Committee for the Purpose of Control and Supervision of Experiments on Animals (CPCSEA), India, with registration number 2165/PO/ReBi/S/22/CPCSEA and protocol number IAEC/SVKM IOP/31.07.2023 (valid for 1 year).

2.6.1 Procurement and maintenance of animals

Male Sprague Dawley rats (180-250 gm) were kept in a controlled environment with regulated humidity and temperature. They were as long as with unrestricted entree to water and a standard pellet diet. The rats were adapted for a week before the experiment began to ensure they were comfortable and accustomed to their surroundings. All procedures were approved and followed strict guidelines throughout the study.

2.6.2 Experimental design

The animal study was conducted with the groups described in Table 3. Group I aided as the normal control and established only the vehicle. Group II, known as the disease control, established only CFA and no treatment. Group III rats were given the disease and treated with a marketed formulation. Group IV was infected with CFA and received the placebo carbopol gel. Group V was infected with CFA and treated with plain DIF gel. Finally, Group VI was infected with CFA and treated with DIF-NS-Gel.

Table 3. Number of groups included in the animal study.

Groups	Name of Group	No. of Animals	Applied Formulations
Group I:	Normal Control	6	Vehicle
Group II:	Diseases control	6	Not Giving Treatment
Group III:	Standard Control	6	Marked Diclofenac Gel
Group IV:	Placebo control	6	Carbopol Gel
Group V:	Plain Gel Control	6	Plain Gel
Group VI:	Formulation Control	6	DIF-NS Gel

2.6.3 CFA (complete Freund's adjuvant) induced arthritis model

Six to seven-week-old male Sprague Dawley rats, with an average weight of 180 ± 20 g, were arbitrarily alienated into four sets, each consisting of six rats. Respectively rat was administered a 0.1 mL injection of CFA into the subplantar region of the left hind paw.

2.6.4 Comprehensive analysis of arthritis progression and treatment efficacy

2.6.4.1 Body weight assessment

The body mass at the preliminary assessment (day 0 before immunization) was nearly the same across all animal groups. Nevertheless, during the ensuing period, the immunized rats dependably had significantly lesser body weights compared to the control rats. In the final week of treatment, the weight of the immunized rats began to approach that of the control rats [35].

2.6.4.2. Hind paw volume assessment

Paw volume measurements were taken to assess the impact of CFA administration on rats. After two weeks of CFA administration, the rats displayed distinct symptoms of rheumatoid arthritis, such as a marked upsurge in paw size, redness, swelling, joint stiffness, and restricted movement illustrated in Fig. 2. Paw volume was measured using a digital plethysmometer on the 1st, 10th, 20th, and 28th day's post-CFA injection. Initially, paw volume measurements (day 0, prior to immunization) were nearly identical across all groups. However, in the subsequent period, paw volume was expressively higher in the immunized rats equated to the control group. By the final week of treatment, the paw volume in immunized rats began to approach the levels observed in control rats [36].

Figure 2. Readings taken on Plethysmometer.

2.6.4.3. Arthritis score

Arthritis severity was assessed visually to gauge walking ability on days 0, 10, 20, and 28. Gait behaviour was evaluated using a modified scale, with scores ranging from 0 to 4: 0 indicating normal walking and running, 1 indicating difficulty, 2 indicating limping without hind paw retraction, 3 indicating limping with hind paw retraction (hind paw not touching the floor), and 4 indicating crawling or lying down. Each arthritic rat had a maximum score of 4.

2.6.4.4 Macroscopic evaluation of CFA-induced arthritis Rats

In the CFA-induced arthritis rat model, we assess macroscopic indicators such as joint swelling, erythema, and deformities to evaluate the progression and severity of arthritis. These visual signs reflect the inflammatory response and tissue damage as characteristic of RA [36].

3. Result and discussion

3.1 Formulation and optimization of DIF-NS

The CCD statistical response surface methodology was employed, providing eleven experimental runs to assess the consequence of two independent variables at predetermined levels on % DD, % EE, PS, and % PY of DIF-NS, as tabulated in Table 4 and Table 5. In Table 5 presents key values that are crucial for optimizing the formulation, showing a difference of less than 0.2 between predicted and adjusted R^2 values, which signifies an excellent fit with the actual model R^2. Additionally, the model's p-values were below 0.05, confirming statistical significance. To further investigate the interactions between variables, 2-D contour plots and 3-D response surface plots were generated from the experimental data. The impact of these independent variables on the responses Y1, Y2, Y3, and Y4 is depicted through 2D and 3D surface plots in Figs. 3(a-d). The strong correlation between experimental data and predicted outcomes

Table 4. Observed values of responses with all batches.

Run	Independent variables (Actual values)		Dependent variables (Actual responses)			
	A (mg)	B (mg)	Y1	Y2	Y3	Y4
1	75	60	89	68	120	73.1
2	100	90	66.8	93.1	175	75.3
3	135.3	90	82	70	190	74.2
4	100	90	65	95	175	76
5	100	47.57	77	81	140	75.5
6	125	120	75	80	210	71
7	100	132.42	70	85	200	59
8	75	120	80.2	75	165	44.1
9	125	60	82.1	73	156	72.8
10	100	90	65.5	93.5	160	74.5
11	64.6	90	91	60	146	54.3

Table 5. Analysis report obtained for three CQAs as per the CCD design.

Response	Model		Lack of fit	R^2	Adjusted R^2	Predicted R^2	Adequate Precision
	F-value	p-value	p-value				
DD (%)	73.17	0.0001	0.2214	0.9865	0.9730	0.9142	23.4006
EE (%)	101.64	< 0.0001	0.2248	0.9903	0.9805	0.9381	27.9830
PS (nm)	75.74	<0.0001	0.8032	0.9498	0.9373	0.9116	23.3873
PY (%)	128.56	< 0.0001	0.1839	0.9923	0.9846	0.9499	31.9639

demonstrates the effectiveness of the design in analyzing and optimizing the formulations. The close alignment of experimental and predicted values further confirms the success of the optimization process.

3.2 Optimization diflunisal nanosponges

The DIF-NS formulation utilized the emulsion solvent evaporation technique. However, in line with quality risk management principles (ICH Q9), it's crucial to acknowledge how independent factors, specific to the product, affect the response variables (CQAs). By employing QRM tools, formulators, and investigators gain an enhanced empathetic of the formulation progression, are facilitating continuous upgrading throughout the product lifecycle.

3.2.1 Effect of independent variables on percentage drug diffusion of drug

The percentage of drug diffusion was observed in the range of 61% to 91%. With the increase in the concentration of EC and PVA, there is a decrease in the drug diffusion through the membrane showing an indirect relationship between each other which is illustrated in Fig. 3(a-d). EC is a hydrophobic polymer that acts as a barrier to water and drug molecules. When the concentration of EC increases, it forms a more impermeable barrier, reducing the rate of drug diffusion through the membrane. This accounts for the observed decrease in drug diffusion with higher EC. When EC and PVA are used together, their interaction can alter the overall structure and properties of the membrane. Here's why a direct relationship between the concentration of the combination and the drug diffusion might be observed. When combined, EC and PVA can form a more complex matrix that balances the hydrophobic and hydrophilic properties. The hydrophobic EC can modulate the swelling behaviour of PVA, potentially creating more uniform and predictable pores in the membrane. This synergy can enhance the diffusion pathways for the drug, leading to an increased rate of drug diffusion compared to when either polymer is used alone at higher concentrations.

$$\%DD = +65.77 - 3.10A - 3.22B + 0.4250AB + 10.76A^2 + 4.26B^2$$

3.2.2 Effect of independent variables on percentage entrapment efficiency

The concentration of ethyl cellulose positively influences the percentage of entrapment efficiency, while the concentration of PVA has a minor positive outcome. The percentage entrapment efficiency ranged from 60% to 95%. The response surface plots, demonstrate how various factors affect entrapment competence. As the concentration of the polymer upsurges, the percentage of entrapment competence also rises. Specifically, higher concentrations of ethyl cellulose lead to greater drug entrapment, and similarly, increased PVA concentration enhances drug entrapment as

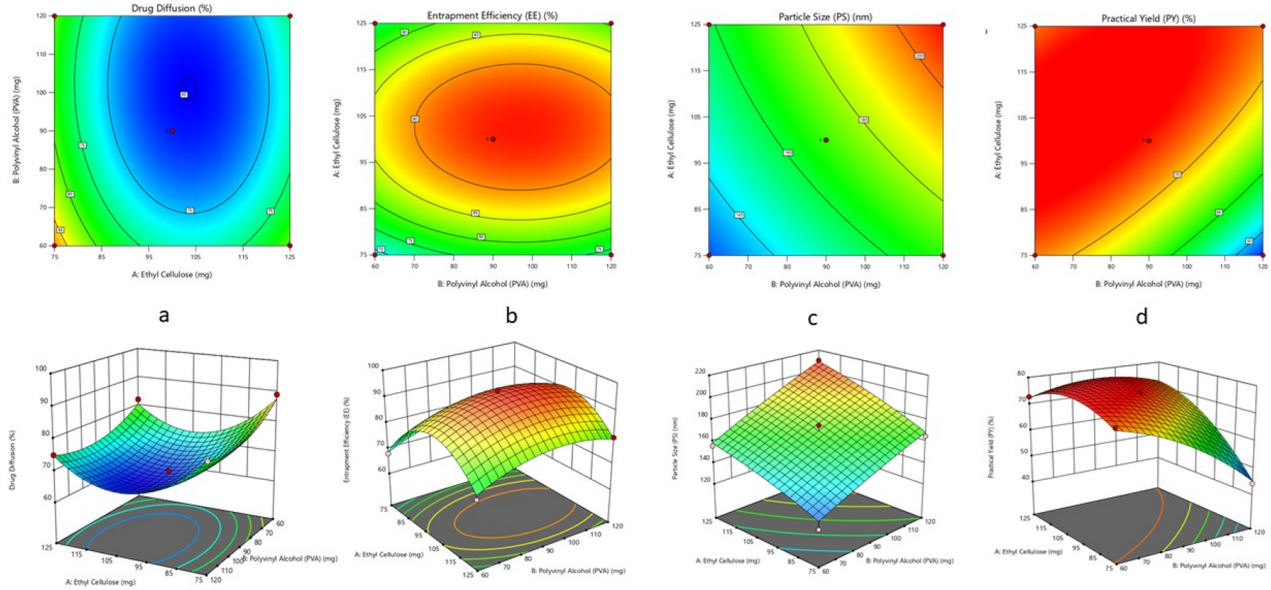

Figure 3. (a-d). 2-D contour plots and 3-D response surface plots showing the influence of CMPs i. e. , (a) EC and (b) PVA onto the percentage Drug Diffusion, percentage entrapment efficiency, particle size and percentage practical. yield.

well. EC is a hydrophobic polymer, which interacts well with hydrophobic drug molecules. Enhanced hydrophobic interactions lead to better incorporation of the drug within the polymer matrix, thus increasing entrapment efficiency. PVA acts as a surfactant and stabilizer, which helps in the formation and stabilization of emulsions during the encapsulation process. Higher PVA concentrations lead to better stabilization of the drug-loaded emulsion droplets, preventing them from coalescing and thus enhancing drug entrapment.

$$\%EE = +93.87 + 3.02A + 2.46B + 0.0000AB - 14.43A^2 - 43B^2$$

3.2.3 Effect of independent variables on particle size

The measured particle sizes varied between 120 nm and 210 nm. A positive correlation between particle size and the concentration of ethyl cellulose is indicated by a positive coefficient in the equation. Conversely, the negative coefficient for PVA suggests an inverse relationship between particle size and this factor. Higher concentrations of ethyl cellulose result in an increase in particle size, likely due to the greater viscidness of the internal phase, which facilitates the formation of larger particles. In contrast, increased concentrations of PVA contribute to system steadiness, lower surface tension, and enhanced steric maintenance of the emulsion, resulting in the production of smaller particles.

$$PS = +170.00 + 17.90A - 22.98B + 2.25AB - 2.56A^2 - 1.56B^2$$

3.2.4 Result of independent variables on percentage practical yield

The practical yield of the nanosponges varied from 44 to 76%, the positive coefficient showing g a positive effect on the practical yield whereas the negative sign of coefficient B showing inverse relationship between Practical yield and concentration of PVA. Increasing the concentration of ethyl cellulose improves the formation of a cohesive and dense polymer matrix. This enhanced matrix formation can encapsulate the drug more effectively and minimize the loss of material during processing, thus increasing the practical yield. While PVA is an effective stabilizer, excessively high concentrations can lead to over-stabilization of the emulsion droplets. Over-stabilization can cause difficulties in the coalescence of droplets necessary for the formation of larger, more manageable particles. This can result in a higher number of fine particles that are lost during processing, reducing the practical yield.

$$\%PY = +75.27 + 6.84A - 6.77B + 6.80AB - 5.63A^2 - 4.13B^2$$

The statistical design of the study included selecting independent variables such as EC and PVA concentrations based on their influence on key Critical Quality Attributes (CQAs) like % Drug Diffusion, % Entrapment Efficiency, and Particle Size. The formulation was optimized using a design approach like Central Composite Design (CCD), enabling the analysis of interactions and quadratic relationships. Statistical tests such as ANOVA, F-values, and p-values were conducted to validate the model and demonstrate the significance of coefficients. The optimization aimed to maximize % EE and % PY while minimizing particle size for optimal performance. Experimental runs validated the model, with high R^2 values indicating a strong correlation between predicted and observed results, confirming the model's predictive reliability.

The optimized Diflunisal nanosponges (DIF-NS) formulation demonstrates superior performance compared to conventional and existing nanoparticle systems. With drug diffusion rates of 61% to 91%, DIF-NS offers enhanced, controlled drug release, outperforming typical tablets and basic nanoparticles that often show limited sustained release. Entrapment efficiency ranges from 60% to 95%, surpassing many polymeric nanoparticle systems due to the effective interaction between ethyl cellulose and PVA. The particle size of 120-210 nm ensures improved bio availability and stability, outperforming larger-sized nanoparticles and conventional formulations. Practical yield rates of 44% to 76% make DIF-NS viable for industrial-scale production, unlike some conventional nanoparticle methods with lower yields. Despite these advantages, further studies are needed to confirm large-scale feasibility and long-term stability.

3.3 Evaluation and characterization of DIF-NS

3.3.1 Fourier transform infrared spectroscopy (FTIR)

The FTIR spectra of DIF, blank NS, and the optimized nanosponge (DIF-NS) are presented in Fig. 4. The DIF spectrum displays characteristic peaks at 3150–3050 cm^{-1} for hydroxyl stretching 1670–1456 cm^{-1} for carbonyl group stretching 1600–1900 cm^{-1} for alkyl bending, and 550–950 cm^{-1} for the alkene bending. Additionally, the functional group peaks of DIF include a fingerprint section spectrum. The peak corresponding to the drug at 3075 cm^{-1} is absent in DIF-NS and shows a shift, indicating electrostatic interactions between the drug and the polymers. While the peak at 1674 cm^{-1} is present in both the pure drug and DIF-NS, it is not observed in the Blank-NS, suggesting drug unloading. Besides, the fingerprint district analysis of drug molecules in DIF-NS reveals augmentation and the vanishing of certain functional peaks, likely due to the encapsulation of the drug.

3.3.2 Differential scanning calorimetry

The thermogram of pure DIF exhibited a distinct endothermic peak at 211 °C, which corresponds to the drug's melting point. On the other hand, the thermogram of the blank nanosponges (placebo) did not display this peak, indicating their amorphous nature. Similarly, the thermogram of DIF-loaded nanosponges (DIF-NS) lacked an endothermic

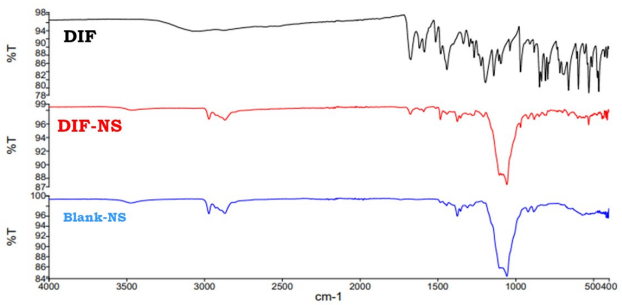

Figure 4. FTIR spectra of pure drug DIF, DIF-NS and Blank-NS.

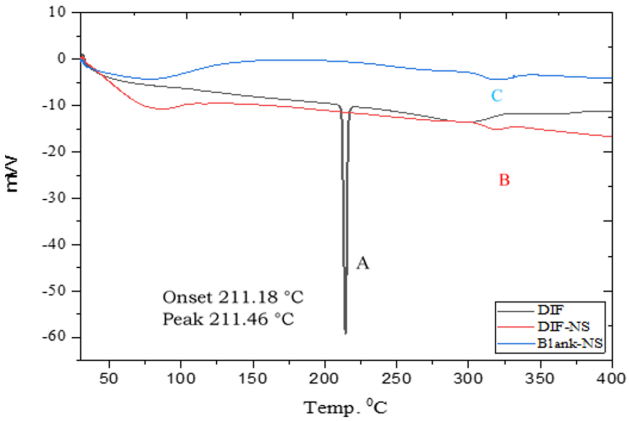

Figure 5. Overlay of thermogram of A-DIF, B-DIF-NS, and C-Blank-NS.

peak, implying the successful encapsulation of the drug within the nanoporous structure of the nanosponges. This suggests a reduction in the drug's crystallinity, likely due to the amorphous characteristics of the nanosponges, as further supported by X-ray diffraction (XRD) analysis illustrated in Fig. 5.

3.3.3 X-ray diffractometry

Typically, a drug's solubility is influenced by its crystalline structure. X-ray diffractogram analysis can reveal whether a compound is crystalline or amorphous. In this investigation, pure DIF exhibited distinct peaks Fig. 6 with the highest intensity reaching 48000 at 2θ angles of 14 °, 15 °, 16 °, 28 °, and 43 °, whereas DIF-NS displayed broader peaks with lower intensity Fig. 6. Sharp, well-defined peaks with high intensity are indicative of a crystalline structure, while broad, low-intensity peaks suggest an amorphous form. The conversion from a crystalline to an amorphous state may improve the solubility and skin penetration of DIF, potentially enhancing its effectiveness in topical applications.

3.3.4 Particle size, PDI, and zeta potential

The particle size and dispersal are risky parameters influencing the constancy and effectiveness of the framed nanosponges for topical permeation. In this study, the selected batch exhibited a particle size of 120.1 ± 8.5 nm and a PDI of 0.348 ± 0.015, as shown in Fig. 7 and Fig. S1. A PDI value below 1 indicates excellent uniformity among the particles. Zeta potential analysis assessed the surface charge of the DIF-NS; stability is generally achieved when the zeta potential is between -30 and +30 mV. The augmented batch exhibited a zeta potential of -29 ± 3.2 mV, as illustrated in Fig. 8 and Fig. S2.

3.3.5 Percentage entrapment efficiency (% EE) and percentage of practical yield (% PY)

The percentage of encapsulation efficiency (% EE) for the augmented batch was assessed by means of a direct method. % EE was determined by measuring the alteration amongst the total amount of DIF added and the amount of entrapped DIF found in the nanosponges. The optimized batch exhibited a % EE of 82.45 % ± 1.2 and a % yield of 75 % ± 2.2.

3.3.6 FESEM (Field emission scanning electron microscopy)

Scanning electron microscopy was utilized to investigate the surface morphology of DIF-NS. The SEM images showed in Figs. 9A and 9B, a spherical shape for DIF-NS and exhibited a porous structure embellished with numerous nanocavities.

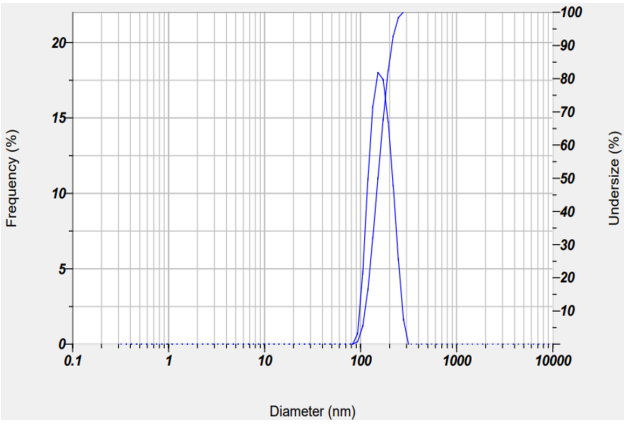

Figure 7. Particle size of the optimized batch.

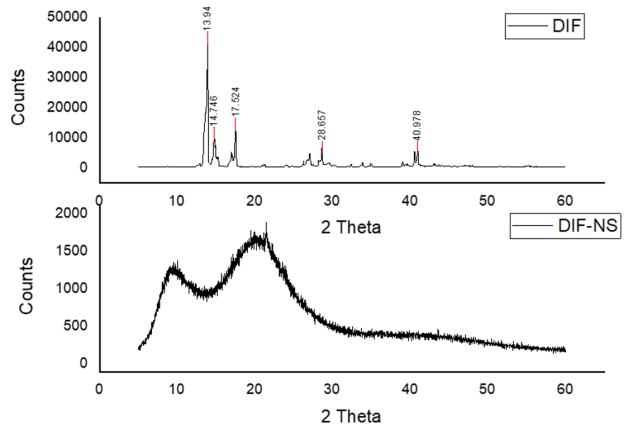

Figure 6. Diffractogram of the DIF and DIF-NS.

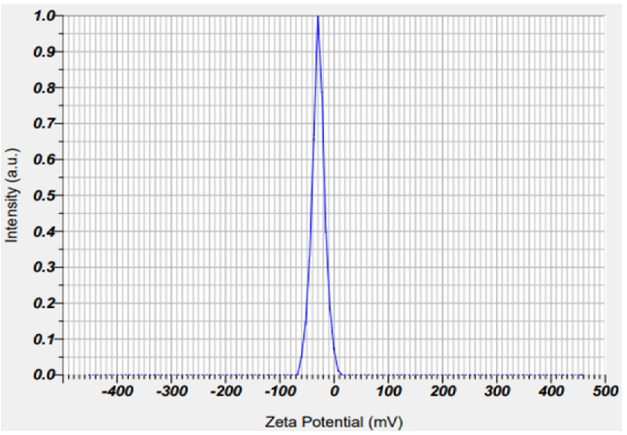

Figure 8. Zeta Potential of optimized batch.

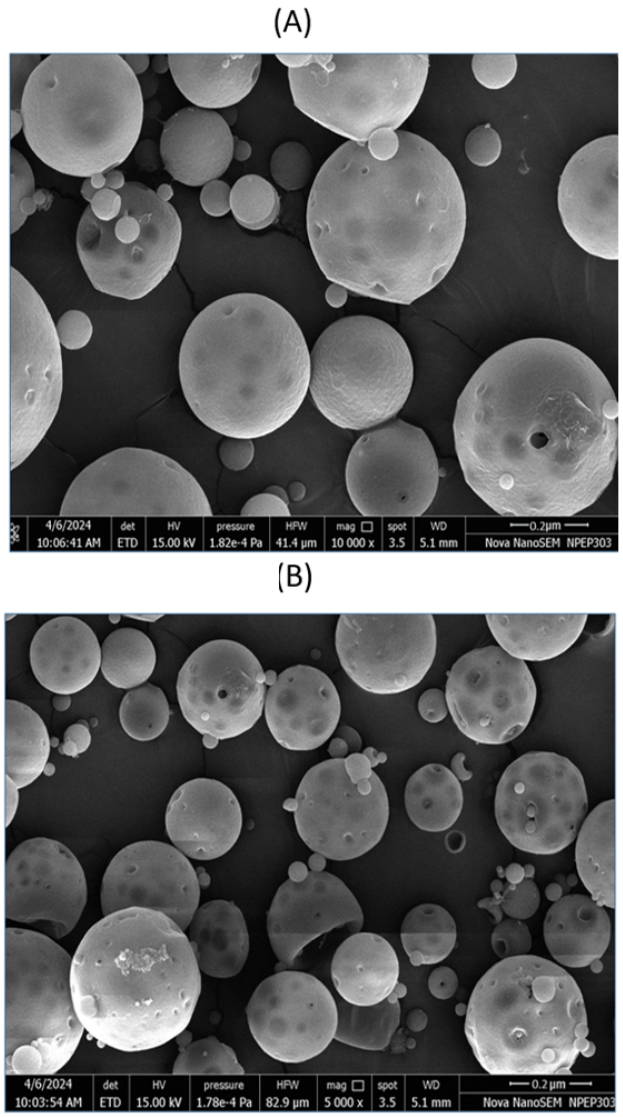

Figure 9. SEM micrographs of optimized nanosponges displaying their surface morphology. (A) DIF-NS at a magnification of 100,000x, revealing a spherical shape with smooth surface characteristics. The uniformity of size distribution can be observed, indicating successful nanosponge formulation with minimal aggregation. (B)DIF-NS at a lower magnification of 5,000x, showing a porous structure with varied particle sizes, highlighting the efficiency of the fabrication process in producing nanosponges with consistent morphology.

3.4 Evaluation of optimized NS-loaded gel

The Carbopol 940P concentration significantly influenced the release of DIF from various DIF-NS-gel. As the Carbopol 940P content increased, the rates of drug release decreased, leading to prolonged drug retention and prevention of leakage for several hours tabulated in Table 6 and Fig. 10. This effect may be ascribed to the viscidness of

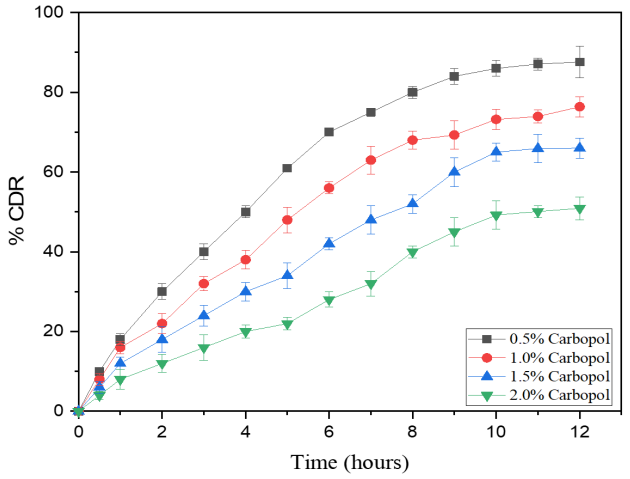

Figure 10. Comparative drug releases from different concentrations of Carbopol Gel drug release profile of the DIF-NS-gel using phosphate buffer solution (pH 7.4) as the release medium at a controlled temperature of 37 ^{O}C to simulate physiological conditions.

the gel at higher Carbopol concentrations, consequential in a finer gel mesh that restricts droplet movement within the gel matrix. The most pronounced impedance of drug release occurred at a 2% Carbopol 940 P concentration. However, below the 0.5 % Carbopol concentration resulted in further enhancement of DIF release. This phenomenon is attributed to Carbopol's ability to form robust gels even at lower concentrations, facilitating the achievement of desired drug release profiles. Table 6 illustrate the selected concentration of Carbopol 940P for optimization of the gel with their optimization parameter. The 1.5 % Carbopol 940 P selected for the further formulation shows a pH of 6.4, viscosity of 26500 cp, spreadability of 16 $\pm$ 0.15 and percentage drug diffusion is 66.65 % respectively.

3.4.1 pH measurement and visual appearance

The pH of the NS-loaded gel containing DIF was assessed using a calibrated digital pH meter (Equip-Tronics digital pH meter model EQ-610). The pH DIF-NS gel was found to be 6.5. The found pH is similar to the skin pH. The formulation underwent assessment for opaque appearances through visual observation against both black and white backgrounds.

3.4.2 Measurement of viscosity

The determination of viscosity was performed by using Brookfield Viscometer on DIF-NS-gel. The viscosity measurements for each formulation and it ranged from the 2600-2660 cp.

Table 6. Optimization results of the gel batches.

Batch	Polymer Used	Con. of Carbopol	pH	Viscosity cp	Spreadability	% DD in 12 hr.
G1	Carbopol 940	0.5	6.8	15000	13 $\pm$ 0.54	87.6
G2	Carbopol 940	1	6.6	23090	14 $\pm$ 0.25	76.36
G3	Carbopol 940	1.5	6.47	26500	16 $\pm$ 0.15	66.65
G4	Carbopol 940	2	6.6	46080	26 $\pm$ 0.35	50.9

3.4.3 Determination of spreadability

To determine gel spreadability, place a defined amount of gel on a horizontal surface. Apply a standard weight on top for a set time. Measure the diameter of the spread area perpendicular to the direction of the applied force. Calculate spreadability using the formula. The nanosponge gel exhibited a spreadability of 5.0 g.cm/sec, suggesting that the spreadability of the drug-loaded nanosponge gel was satisfactory.

3.4.4 In vitro drug release study

The *In vitro* drug release study of plain drug Gel, DIF-NS loaded in the gel was performed. An *In vitro* drug release investigation was achieved by using a Franz diffusion cell. The plain drug exhibits only 73.1 ± 3.5 drug releases due to its classification as a BCS class II drug, considered by low solubility and high permeability. Furthermore, the optimized DIF-NS gel exhibits a % CDR of 84.9 ± 1.6 within 12 hours. Notably, when NS is loaded in gel, the drug release is further maximum with high permeation as compared to plain drug gel alone, likely due to the incorporation of NS within a thick viscous gel matrix illustrated in Fig. 11.

3.4.5 Ex-vivo permeation study

The *Ex-vivo* permeation investigation was directed to evaluate the concert of the optimized DIF-NS-gel formulation and a plain DIF gel on rat skin. The persistence of this study was to inspect how effectively the two different gel formulations could deliver the drug through the skin, which is an essential factor for ensuring therapeutic efficacy in topical treatments. Results from the study revealed that, within a 12-hour period, the optimized DIF-NS-gel formulation exhibited a drug permeation rate of 90.78 ± 2.7. This rate was significantly higher compared to the permeation rate of 65.29 ± 3 observed for the plain DIF gel at the same time point. The substantial difference in drug permeation rates between the two formulations highlights the superior performance of the optimized DIF-NS-gel. One possible explanation for this disparity is the slow release mechanism inherent in the plain gel formulation. The plain gel's drug release is further regulated by the gelling matrix of the polymer used in its composition illustrated in Fig. 12.

For clinical practice, the implications of these findings are notable. The enhanced permeation and controlled release profile of the DIF-NS-gel can potentially reduce the frequency of application required, thus improving patient compliance. Sustained drug release may lead to more consistent pain relief and inflammation control, minimizing the peaks and troughs associated with conventional topical applications. This could help in maintaining therapeutic drug levels over extended periods, leading to better disease management and reduced systemic exposure. In the context of rheumatoid arthritis treatment, where chronic pain and inflammation require effective long-term management, the prolonged action of the DIF-NS-gel offers a promising strategy. It may allow patients to experience sustained symptom relief without the need for frequent reapplication, thereby enhancing the quality of life and adherence to treatment regimens. Further clinical trials would be necessary to confirm these benefits and assess long-term safety and efficacy in human subjects.

3.4.6 Release kinetics

The release data from the optimized batch was analyzed using various kinetic models, including zero-order, first-order, Higuchi, Korsmeyer-Peppas, and Hixson-Crowell models. The Higuchi model, based on Fick's law of diffusion, and the Korsmeyer-Peppas model, which describes drug release from polymeric systems are following a Quasi-Fickian diffusion mechanism, were key focuses. The goodness of fit for these models was determined through the coefficient of determination (R^2). The analysis revealed that the Higuchi model best described the release behavior of DIF-NS-gel, showing a strong correlation with an R^2 value of 0.988.

3.4.7 Stability study

The stability assessment of the DIF-NS topical gel batch NS-4 was achieved to estimate the possessions of formulation additives on DIF stability and determine the formulation's physical stability. The stability study included various storage conditions and temperatures. The optimized batch

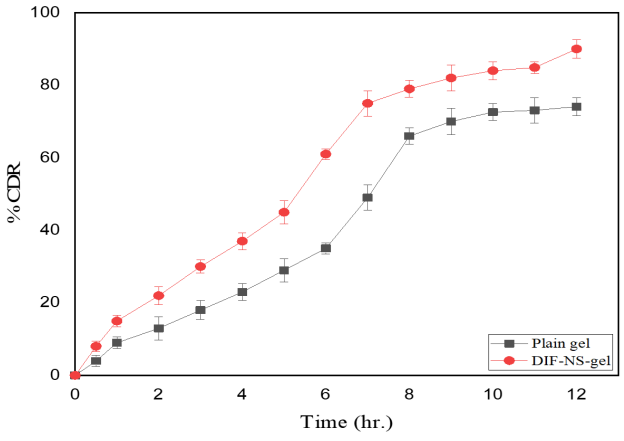

Figure 11. Comparative in vitro drug release profile of plain DIF gel and optimized DIF-NS gel using phosphate buffer solution (pH 7.4) as the release medium at 37 ^{O}C, mimicking physiological temperature conditions for drug release over a 12-hour period.

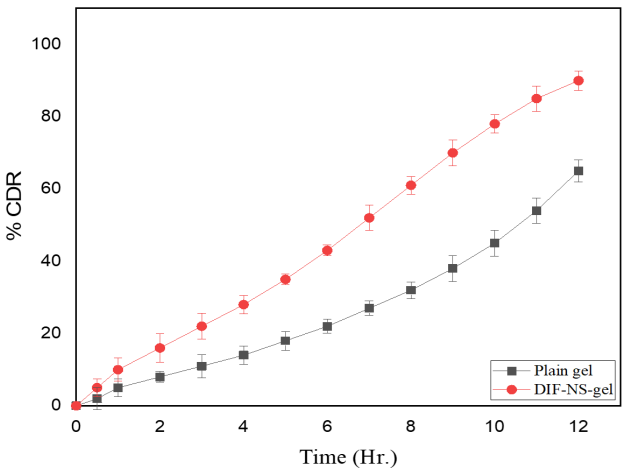

Figure 12. Ex-Vivo Comparative drug releases of plain gel and DIF-NS-Gel.

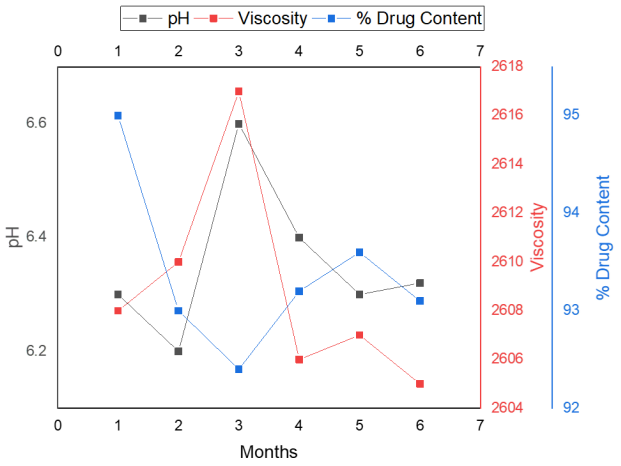

Figure 13. Stability profile of the optimized DIF-NS gel (batch NS-4) under accelerated stability conditions at 40 ^{O}C ± 2 ^{O}C / 75% RH ± 5% RH, with evaluations at 1, 2, 4, and 6 months.

formulation was exposed to accelerated stability condition 40 ^{O}C ± 2 ^{O}CC / 75% RH ± 5% RH as well as in photostability chamber. Samples were collected at specific intervals (1, 2, 4, and 6 month) for physical evaluation, including measurements of pH, colour, odour, viscosity and drug content. There is no change in the colour and odour of the DIF-NS gel shown in Fig. 13 and Fig. 14.

3.5 Animal study

3.5.1 Comprehensive analysis of arthritis progression and treatment efficacy

3.5.1.1 Body weight assessment

The effect of Body Weight on diclofenac marketed gel, plain Carbopol gel, plain DIF gel, and DIF-NS gel on the CFA-immunized rats was tested for CFA-induced rheumatoid arthritis. Application of two-way ANOVA showed significant changes in body weight on day 0, day 10, day 20, and day 28 with the different group [F (5, 120) = 8.262, p < 0.01] Fig. 15. Bonferroni's post hoc multiple comparisons test showed a significant change from day 20 in body weight of CFA-induced rheumatoid arthritis as compared to the control (p < 0.01). On day 20 the body weight of the Diclofenac as a standard group (p < 0.05), and DIF-NS-

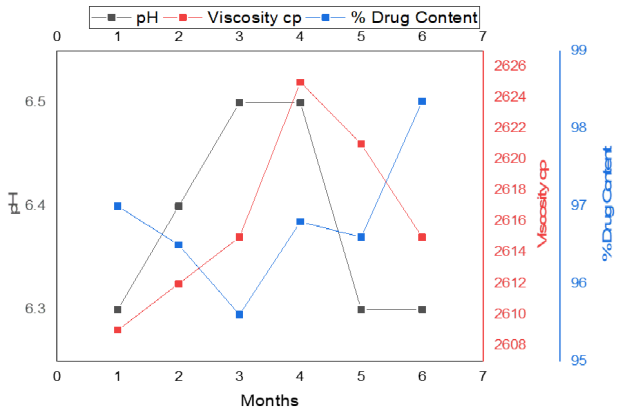

Figure 14. Stability graph in photostability condition.

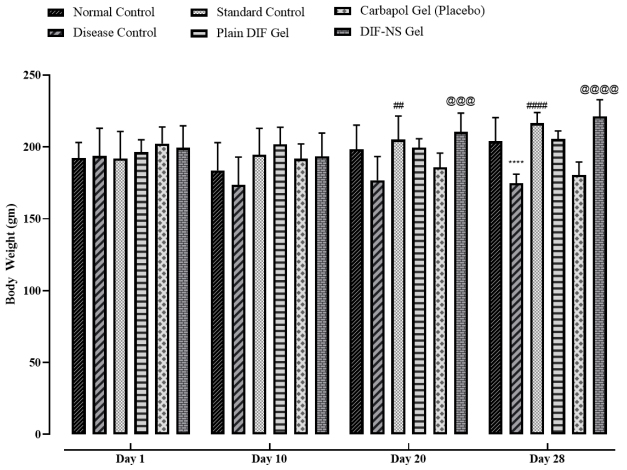

Figure 15. Effect of DIF-NS-Gel on CFA-Immunized RA rat on body weight.The data were analyzed using two-way ANOVA followed by Bonferroni's post hoc multiple comparison test. All the values were expressed as mean ± SEM. **** P < 0.0001 CFA-Immunized rheumatoid arthritis v/s normal control group; CFA-Immunized rheumatoid arthritis v/s Diclofenac treatment group #### P < 0.0001, DIF-NS-Gel group @@@@ P < 0.01.

Gel group (p < 0.01) significantly increased body weight. Furthermore, on day 28, the standard group as a Diclofenac treatment group (p < 0.01), the DIF-NS-Gel group (p < 0.001), significantly showed an increase in body weight and other groups such as Carbopol placebo, Plain DIF gel showed non-significant data (p > 0.05). This suggests the effectiveness of the DIF-NS-Gel group in improving Body weight in CFA-induced arthritis.

3.5.1.2 Hind paw volume assessment

The effect of Hind paw volume assessment on diclofenac marketed gel, plain Carbopol gel, plain DIF gel, and DIF-NS gel on the CFA-immunized rats was tested for CFA-induced rheumatoid arthritis. Application of two-way ANOVA showed significant changes in Hind Paw Volume on day 0, day 10, day 20, and day 28 with the different group [F (5, 120) = 15.66, p < 0.0001] Fig. 16. Bonferroni's post

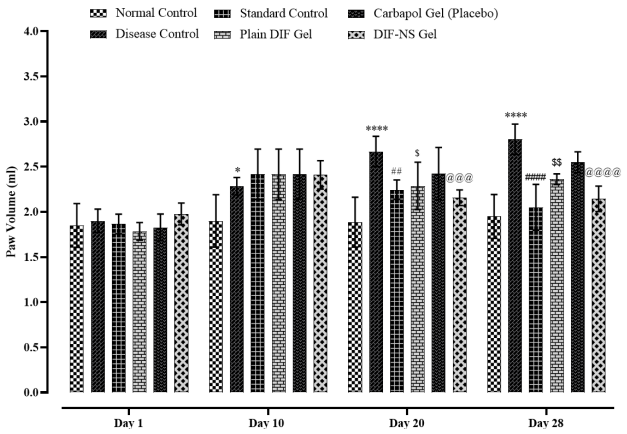

Figure 16. Effect of DIF-NS-Gel on CFA-Immunized rheumatoid arthritis rat on Hind paw volume assessment. The data were analyzed by means of two-way ANOVA tracked by Bonferroni's post hoc multiple comparison test. All the values were expressed as mean ± SEM. CFA-Immunized rheumatoid arthritis v/s normal control group **** P < 0.0001; CFA-Immunized rheumatoid arthritis v/s Diclofenac treatment group #### P < 0.0001, DIF-NS-Gel group @@@@ P < 0.0001, Plain-DIF Gel $$P < 0.01.

hoc multiple comparisons test showed a significant change from day 10 in Hind Paw Volume of CFA-induced rheumatoid arthritis as compared to the control ($p < 0.05$) and from day 20 ($p < 0.0001$). On day 20 the Hind paw volume of the Diclofenac as a standard group ($p < 0.01$), and the DIF-NS-Gel group ($p < 0.001$) significantly reduced hind paw volume as compared to CFA-induced rheumatoid arthritis. Furthermore, on day 28, the standard group as a Diclofenac treatment group ($p < 0.0001$), the DIF-NS-Gel group ($p < 0.001$), DIF-Plain Gel ($p < 0.01$) significantly showed a reduced in paw volume and another group such as Carbopol placebo, showed non-significant data ($p > 0.05$). This suggests the effectiveness of the DIF-NS-Gel group in reducing Hind-paw volume in CFA-induced arthritis.

3.5.1.3 Arthritis score

The effect of Arthritis score on diclofenac marketed gel, plain Carbopol gel, plain DIF gel, and DIF-NS gel on the CFA-immunized rats was tested for CFA-induced rheumatoid arthritis illustrated in Fig. 16. Application of two-way ANOVA showed significant changes in Arthritis score on day 0, day 10, day 20, and day 28 with the different group [$F(5, 120) = 64.79$, $p < 0.0001$] Fig. 17. Bonferroni's post hoc multiple comparisons test showed a significant change from day 20 in the Arthritis score of CFA-induced rheumatoid arthritis as compared to the control ($p < 0.0001$). On day 20 the arthritis score of the Diclofenac as a standard group ($p < 0.01$), and DIF-NS-Gel group ($p < 0.01$) significantly modulate arthritis score as compared to CFA-induced rheumatoid arthritis. Furthermore, on day 28, the standard group as a Diclofenac treatment group ($p < 0.0001$), the DIF-NS-Gel group ($p < 0.0001$), DIF-Plain Gel ($p < 0.001$) significantly showed a reduced arthritis group and another group such as Carbopol placebo, showed non-significant data ($p > 0.05$). This suggests the effectiveness of the DIF-NS-Gel group in modulating Arthritis scores in CFA-induced arthritis.

3.5.1.4 Factorial factors effect in details with comparison from literature

The efficacy of drug formulations such as the DIF-NS gel can be profoundly influenced by multiple factors that contribute to their therapeutic outcomes. The concentration of the drug and polymer components in the formulation, such as Carbopol 940P, plays a critical role. Higher polymer concentrations typically result in increased gel viscosity, leading to a slower drug release due to the denser gel matrix, as seen in both your study and corroborated by recent literature. This effect optimizes sustained release and prolonged drug retention. Additionally, the zeta potential is a crucial parameter in assessing colloidal stability. Formulations with optimal zeta potential prevent particle aggregation, ensuring uniform drug distribution and release over time [37]. The research into various nanoscale delivery systems for rheumatoid arthritis has shown that optimized formulations not only prolong drug release but also enhance bioavailability compared to non-nano drug forms. In vivo studies, particularly using CFA-induced arthritis models, provide essential insights into how these formulations perform under physiological conditions. Measurements of body weight, paw swelling, and arthritis scores are significant indicators of disease progression and treatment efficacy. Recent literature supports that nanoformulations exhibit superior performance in reducing inflammation and improving overall health markers, aligning with findings from your study that indicated significant improvements in body weight and hind paw volume with the DIF-NS gel treatment. Statistical analysis using robust methods such as two-way ANOVA and post hoc tests confirms the reliability of these results, ensuring that observed differences between treatment groups are statistically significant and not due to random variation. This comprehensive approach underscores the importance of factorial analysis in the optimization of drug formulations, as it ensures that each variable's contribution to the outcome is adequately evaluated [38].

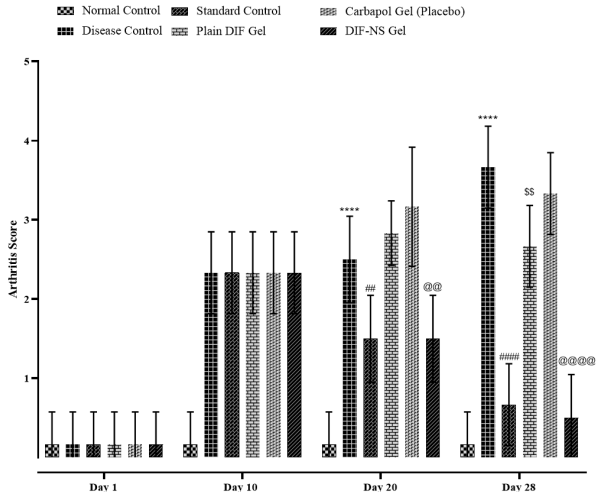

Figure 17. Effect of DIF-NS-Gel on CFA-Immunized rheumatoid arthritis rat on arthritis score.The data were analysed by means of two-way ANOVA tracked by Bonferroni's post hoc multiple comparison tests. All the values were expressed as mean ± SEM. CFA-Immunized rheumatoid arthritis v/s normal control group **** P ¡ 0.0001; CFA-Immunized rheumatoid arthritis v/s Diclofenac treatment group #### P < 0.0001, DIF-NS-Gel group @@@@ P < 0.0001, Plain-DIF Gel $$ P < 0.01.

3.5.1.5 Macroscopic evaluation of CFA-induced arthritis Rats

In the CFA-induced arthritis rat model, we assess macroscopic indicators such as joint swelling, erythema, and deformities to evaluate the progression and severity of arthritis. These visual signs reflect the inflammatory response and tissue damage characteristic of rheumatoid arthritis. The 28-day protocol to evaluate the anti-rheumatic activity was successfully completed using six groups: I-Normal group, II-Disease induced group, III-Standard control, IV-Placebo control, V-Plain gel control, and VI-Formulation control. Figs. 18 illustrate that significant differences in swelling were observed between the Disease induced and formulation control groups, indicating the formulation's efficacy. By the end of the study, the Formulation control group showed swelling levels comparable to the Normal group, suggesting effective mitigation of disease symptoms. The Standard control group exhibited a slight swelling, even after the study's completion. In contrast, the placebo control group continued to show swelling after 28 days, while the plain gel control group only experienced a slight reduction in swelling, highlighting the specific therapeutic benefit of the formulated drug.

Figure 18. Monitoring of the swelling and comparison between the I-Normal group, II- Disease induced groups, III- Standard Control, IV-Placebo Control, V-Plain Gel Control and VI – Formulation Control after 28 days.

4. Conclusion

The study concluded that joint swelling, deformities, and erosion are primary manifestations of rheumatoid arthritis, a prevalent chronic inflammatory disease affecting 0.5% to 1% of adults worldwide. Effective management and timely diagnosis are crucial for alleviating symptoms and preventing complications. DIF, new semisynthetic non-steroidal anti-inflammatory drugs (NSAIDs), shows anti-inflammatory effects and is used for pain management in rheumatoid arthritis, though it has the disadvantage of anti-platelet activity in tablet form. This underscores the need for a topical formulation that bypasses systemic circulation. The study developed a nanosponge-based topical formulation using the Emulsion solvent diffusion Method to enhance skin permeation. The formulation involved various drug-polymer ratios, with compatibility confirmed through FTIR and characterization by multiple analytical methods. Optimized through Central Composite Design, the NS-4 batch demonstrated desirable properties with a 0.976 desirability value. The NS-4 batch showed significant improvements in % DD, % EE, particle size, and % PY, with DSC confirming drug entrapment and XRD indicating reduced crystallinity. SEM revealed an appropriate nanosponge structure, and In vitro studies showed a 90.78% drug release over 12 hours. Ex-vivo and stability studies confirmed the formulation's efficacy and stability. Animal studies indicated significant mitigation of anti-rheumatic symptoms, suggesting the developed topical DIF delivery system enhances permeability and therapeutic efficacy, reducing oral side effects. The study successfully developed an optimized nanosponge-based topical formulation of diflunisal, demonstrating improved skin permeation, stability, and therapeutic efficacy compared to traditional delivery methods. Future work could include clinical trials to confirm its safety and effectiveness, as well as further refinement to enhance patient outcomes and broader applications.

Authors contributions
Authors have contributed equally in preparing and writing the manuscript.

Availability of data and materials
The authors declare that the data supporting the findings of this study are available within the paper.

Conflict of interests
The authors assert that they do not have any identifiable conflicting financial interests or personal relationships that might be perceived to influence the work presented in this paper.

Funding statement The authors sincerely thank Shri Vile Parle Kelavani Mandal's Institute of Pharmacy, Dhule, Maharashtra (India) for providing SEED grant funding, which helped us to complete this research work.

References

[1] R. Khurana and S. M. Berney. " Clinical aspects of rheumatoid arthritis.". *Pathophysiology*, 12:153–165, 2005.
DOI: https://doi.org/10.1016/J.PATHOPHYS.2005.07.009.

[2] R. Handa, U. R. K. Rao, J. F. M. Lewis, G. Rambhad, S. Shiff, and C. J. Ghia. "Literature review of rheumatoid arthritis in India.". 2015.
DOI: https://doi.org/10.1111/1756-185X.12621.

[3] F. Wang, J. Liu, Y. Fang, J. Wen, M. He, Q. Han, and X. Li. "Hypercoagulability in rheumatoid arthritis: A bibliometric analysis and retrospective data mining study.". *ACS Omega*, 8:48522–48534, 2023.

[4] D. M. Lee and M. E. Weinblatt. "Rheumatoid arthritis.". *Lancet*, 358:903–911, 2001.
DOI: https://doi.org/10.1016/S0140-6736(01)06075-5.

[5] K. Almutairi, J. Nossent, D. Preen, H. Keen, and C. Inderjeeth. "The global prevalence of rheumatoid arthritis: a meta-analysis based on a systematic review.". *Rheumatol Int*, 41:863–877, 2021.
DOI: https://doi.org/10.1007/S00296-020-04731-0.

[6] J. S. Smolen, D. Aletaha, and I. B. McInnes. "Rheumatoid arthritis.". *Lancet*, 388:2023–2038, 2016.
DOI: https://doi.org/10.1016/S0140-6736(16)30173-8.

[7] B. M. Khler, J. Gunther, D. Kaudewitz, and H. M. Lorenz. " Current Therapeutic Options in the Treatment of Rheumatoid Arthritis.". *J Clin Med*, 8, 2019.
DOI: https://doi.org/10.3390/JCM8070938.

[8] M. A. Sallam, A. M. Motawaa, and S. M. Mortada. "An insight on human skin penetration of diflunisal: lipogel versus hydrogel microemulsion.". *Drug Dev Ind Pharm*, 41:141–147, 2015.
DOI: https://doi.org/10.3109/03639045.2013.850711.

[9] S. Bindu, S. Mazumder, and U. Bandyopadhyay. "Non-steroidal anti-inflammatory drugs (NSAIDs) and organ damage: A current perspective.". *Biochem Pharmacol*, 180, 2020.
DOI: https://doi.org/10.1016/J.BCP.2020.114147.

[10] M. Habeeb, H. Woon You, K. Balasaheb Aher, G. Balasaheb Bhavar, S. Suryabhan Pawar, and S. Dnyaneshwar Gaikwad. "Artificial neural networks for the prediction of mechanical properties of CGNP/PLGA nanocomposites.". *Mater Today Proc*, 2023.
DOI: https://doi.org/10.1016/J.MATPR.2023.08.354.

[11] M. Habeeb, S. Arsey, H. W. You, S. T. Kumbhar, K. B. Aher, G. B. Bhavar, and H. T. Vengateswaran. "Targeted nanomedicine modulating intercellular communications to arrest renal cell carcinoma progression.". *J Drug Deliv Sci Technol*, 99:105983, 2024.
DOI: https://doi.org/10.1016/J.JDDST.2024.105983.

[12] H. Mohammad, H. W. You, M. Umapathi, K. K. Ravikumar Hariyadi, and S. Mishra. "Strategies of Artificial intelligence tools in the domain of nanomedicine.". *J Drug Deliv Sci Technol*, page 105157, 2023.
DOI: https://doi.org/10.1016/J.JDDST.2023.105157.

[13] H. T. Vengateswaran, M. Habeeb, K. B. Aher, G. B. Bhavar, P. Suseela, and I. Navabshan. "Radiant revolution with carbon dots transforming medicine.". *Futuristic Trends in Chemical Material Sciences & Nano Technology Volume*, 5:59–70, 2024.
DOI: https://doi.org/10.58532/V3BECS5P1CH6.

[14] M. S. Sadjadi, B. Sadeghi, and K. Zare. "Natural bond orbital (NBO) population analysis of cyclic thionylphosphazenes, [NSOX $(NPCl_2)_2$]; X = F (1), X = Cl (2).". *Journal of Molecular Structure: THEOCHEM*, 817:27–33, 2007.
DOI: https://doi.org/10.1016/J.THEOCHEM.2007.04.015.

[15] M. A. S. Sadjadi, M. Meskinfam, B. Sadeghi, H. Jazdarreh, and K. Zare. "In situ biomimetic synthesis and characterization of nano hydroxyapatite in gelatin matrix.". *J Biomed Nanotechnol*, 7:450–454, 2011.
DOI: https://doi.org/10.1166/JBN.2011.1305.

[16] B. Sadeghi, S. H. Ghammamy, Z. Gholipour, M. Ghorchibeigy, and A. A. Nia. "Gold/hydroxypropyl cellulose hybrid nanocomposite constructed with more complete coverage of gold nano-shell.". *Micro Nano Lett*, 6:209–213, 2011.
DOI: https://doi.org/10.1049/MNL.2011.0036.

[17] A. Amininia, K. Pourshamsian, and B. Sadeghi. " Nano-ZnO impregnated on starch—A highly efficient heterogeneous bio-based catalyst for one-pot synthesis of pyranopyrimidinone and xanthene derivatives as potential antibacterial agents.". *Russian Journal of Organic Chemistry*, 56:1279–1288, 2020.
DOI: https://doi.org/10.1134/S1070428020070234/METRICS.

[18] B. Sadeghy and S. Ghammami. "Oxidation of alcohols with tetramethylammonium fluorochromate in aceticoi acid.". *Russ J Gen Chem*, 75:1886–1888, 2005.
DOI: https://doi.org/10.1007/S11176-006-0008-0/METRICS.

[19] M. Habeeb, T. A. Kareem, K. L. Deepthi, V. S. Khot, Y. H. Woon, and S. S. Pawar. "Nanomedicine for targeting the lung cancer cells by interpreting the signaling pathways.". *J Drug Deliv Sci Technol*, 77:103865, 2002.
DOI: https://doi.org/10.1016/J.JDDST.2022.103865.

[20] K. Rodrigues, S. Nadaf, N. Rarokar, N. Gurav, P. Jagtap, P. Mali, M. Ayyanar, M. Kalaskar, and S. Gurav. "QBD approach for the development of hesperetin loaded colloidal nanosponges for sustained delivery: In-vitro, ex-vivo, and in-vivo assessment.". *OpenNano*, 7: 100045, 2010.
DOI: https://doi.org/10.1016/J.ONANO.2022.100045.

[21] U. S. Bagul, M. V. Nazirkar, A. K. Mane, S. V. Khot, A. A. Tagalpallewar, and C.R. Kokare. "Fabrication of architectonic nanosponges for intraocular delivery of Brinzolamide: An insight into QbD driven optimization, in vitro characterization, and pharmacodynamics.". *Int J Pharm*, 650, 2024.
DOI: https://doi.org/10.1016/J.IJPHARM.2023.123746.

[22] M. Habeeb, H. T. Vengateswaran, H. W. You, and K. B. Aherand G. B. Bhavarand S. D. Gaikwad. "Development and characterization of carboxylated copper oxide conjugated polymeric nanocomposites and correlating with computational techniques.". *Results in Surfaces and Interfaces*, 17:100323, 2024.
DOI: https://doi.org/10.1016/J.RSURFI.2024.100323.

[23] A. Salawi, M. Alam, M. Zaman, S. Qureshi, S. S. Shah, I. Majeed, U. Farooq, W. Mustafa, Q. ul, A. Shamim, W. Siddique, Y. Almoshari, and M. Alshamrani. "Optimization and fabrication of the nanosponge carriers of on dansetron using one-factor design.". *Pak J Pharm Sci*, 35:1135–1142, 2022.
DOI: https://doi.org/10.36721/PJPS.2022.35.4.REG.1135-1142.1.

[24] B. Pyrak, K. Rogacka-Pyrak, T. Gubica, and L. Szeleszczuk. "Exploring cyclodextrin-based nanosponges as drug delivery systems: understanding the physicochemical factors influencing drug loading and release kinetics.". *Int J Mol Sci*, 25, 2024.
DOI: https://doi.org/10.3390/IJMS25063527.

[25] A. Kanugo, A. Deshpande, and R. Sharma. "Formulation optimization and evaluation of nanocochleate gel of famciclovir for the treatment of herpes zoster.". *Recent Pat Nanotechnol*, 17:259–269, 2023.
DOI: https://doi.org/10.2174/1872210516666220622115553.

[26] S. Sharma, A. Kanugo, T. Kaur, and D. Choudhary. "Formulation and characterization of self-microemulsifying drug delivery system (SMEDDS) of sertraline hydrochloride.". *Recent Pat Nanotechnol*, 18:3–16, 2022.
DOI: https://doi.org/10.2174/1872210516666220623152440.

[27] T. Dugad and A. Kanugo. "Design optimization and evaluation of solid lipid nanoparticles of azelnidipine for the treatment of hypertension.". *Recent Pat Nanotechnol*, 18:22–32, 2022.
DOI: https://doi.org/10.2174/1872210517666221019102543.

[28] G. A. El-Emam, G. N. S. Girgis, M. M. A. El Sokkary, O. A. El-Azeem Soliman, and A. E. G. H. Abd El Gawad. " Ocular inserts of voriconazole-loaded proniosomal gels: formulation, evaluation and microbiological studies.". *Int J Nanomedicine*, 15:7825–7840, 2020.
DOI: https://doi.org/10.2147/IJN.S268208.

[29] A. Kaur, B. S. Bhoop, S. Chhibber, G. Sharma, V. S. Gondil, and O. P. Katare. "Supramolecular nano-engineered lipidic carriers based on diflunisal-phospholipid complex for transdermal delivery: QbD based optimization, characterization and preclinical investigations for management of rheumatoid arthritis.". *Int J Pharm*, 533:206–224, 2017.
DOI: https://doi.org/10.1016/J.IJPHARM.2017.09.041.

[30] S. H. Abd El-Alim, A. A. Kassem, M. Basha, and A. Salama. "Comparative study of liposomes, ethosomes and transfersomes as carriers for enhancing the transdermal delivery of diflunisal: In vitro and in vivo evaluation.". *Int J Pharm*, 563:293–303, 2019.
DOI: https://doi.org/10.1016/J.IJPHARM.2019.04.001.

[31] S. Sharma, A. Kanugo, and J. Gaikwad. "Design and development of solid lipid nanoparticles of tazarotene for the treatment of psoriasis and acne: a quality by design approach.". *Materials Technology*, 37: 735–744, 2022.
DOI: https://doi.org/10.1080/10667857.2021.1873637.

[32] J. Song and Z. Zhang. "Brinzolamide loaded core-shell nanoparticles for enhanced coronial penetration in the treatment of glaucoma.". *J Appl Biomater Funct Mater*, 18, 2020.
DOI: https://doi.org/10.1177/2280800020942712.

[33] M. M. Obiedallah, A. M. Abdel-Mageed, and T. H. Elfaham. "Ocular administration of acetazolamide microsponges in situ gel formulations.". *Saudi Pharm J*, 26:909–920, 2018.
DOI: https://doi.org/10.1016/J.JSPS.2018.01.005.

[34] S. Nurman, R. Yulia, Irmayanti, E. Noor, and T. C. Sunarti. "The optimization of gel preparations using the active compounds of arabica coffee ground nanoparticles.". *Scientia Pharmaceutica*, 87:32, 2019.
DOI: https://doi.org/10.3390/SCIPHARM87040032.

[35] X. Cui, R. Wang, P. Bian, Q. Wu, V. D. D. Seshadri, and L. Liu. "Evaluation of antiarthritic activity of nimbolide against Freund's adjuvant induced arthritis in rats.". *Artif Cells Nanomed Biotechnol*, 47:3391–3398, 2019.
DOI: https://doi.org/10.1080/21691401.2019.1649269.

[36] S. R. Jitta, P. Daram, K. Gourishetti, C. S. Misra, P. R. Polu, A. Shah, C. S. Shreedhara, M. Nampoothiri, and R. Lobo. "Terminalia tomentosa bark ameliorates inflammation and arthritis in carrageenan induced inflammatory model and freund's adjuvant-induced arthritis model in rats.". *J Toxicol*, 2019.
DOI: https://doi.org/10.1155/2019/7898914.

[37] H. J. Kassab, H. K. Alkufi, and L. S. Hussein. "Use of factorial design in formulation and evaluation of intrarectal in situ gel of sumatriptan.". *J Adv Pharm Technol Res*, 14:119, 2023.
DOI: https://doi.org/10.4103/JAPTR.JAPTR_603_22.

[38] H. Elmotasem and G. E. A. Awad. "A stepwise optimization strategy to formulate in situ gelling formulations comprising fluconazole-hydroxypropyl-beta-cyclodextrin complex loaded niosomal vesicles and Eudragit nanoparticles for enhanced antifungal activity and prolonged ocular delivery.". *Asian J Pharm Sci*, 15:617–636, 2020.
DOI: https://doi.org/10.1016/J.AJPS.2019.09.003.